Electromagnetic scattering by breaking waves: an hp-Adaptive Finite Element approach.

Arnaud Coatanhay
Lab-STICC UMR 6285, ENSTA Bretagne
2 rue François Verny
29806 Brest Cedex 9, France
Email: arnaud.coatanhay@ensta-bretagne.fr

***Abstract*—This article deals with the simulation of the electromagnetic field scattered by sea breaking waves using fluid mechanic theory and hp-Adaptive Finite Element approach. This exterior Maxwell problem is also based upon the use of infinite elements.**

I. INTRODUCTION

For remote sensing applications, many studies have been developed to numerically simulate the radar cross section of the sea surfaces in various weather conditions and with different frequency bands. For low wind speed and in deep sea, the surface can be easily described by linear models and electromagnetic simulations based upon asymptotic approaches or numerical boundary element methods (Methods of Moments) are proved to be very efficient. For higher wind speed and for coastal area, sea surfaces become non-linear and induce complex shape: breaking waves. From electromagnetic point of view, the profile of a breaking wave must be considered as a complex target, see figure 1, that raises some important issues for numerical convergence.

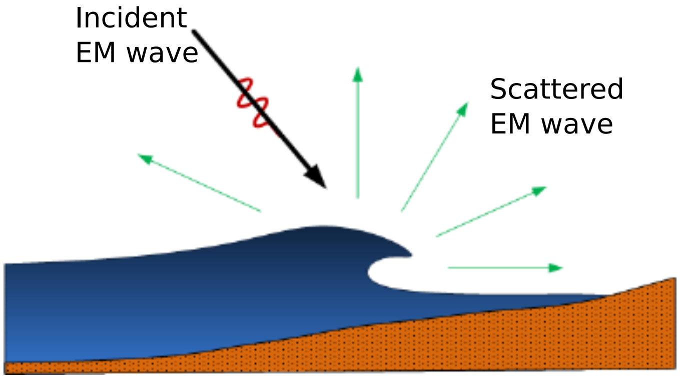

Fig. 1. Scattering by a coastal breaking wave.

II. PHYSICAL AND NUMERICAL MODELS

To obtain reliable simulations of the electromagnetic scattering by a breaking wave, we must manage the both aspects of the set problem: fluid mechanics and electromagnetic issues.

A. Breaking wave model

The breaking waves are described by strongly non-linear Navier-Stokes equations and many approaches (boundary element methods, Finite Differences,...) can be applied to compute numerical simulation [1]. Nevertheless, standard methods remains very time consuming.

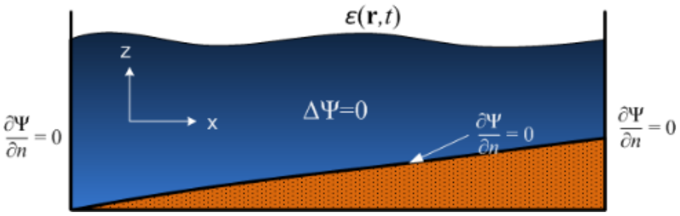

Fig. 2. Fluid modeling.

Assuming an incompressible and irrotational fluid, the sea waves can be described using the velocity potential Ψ. In this case, potential Ψ satisfies the homogeneous Laplacian equation and the homogeneous Neumann boundary conditions (static boundaries), see figure 2. The sea surface is a free boundary. Using a desingularized technique [2], [3], [4] combined with conformal transformations [5], the differential equation can be efficiently solved. The initial conditions are provided by a static Gaussian profile, see figure 3

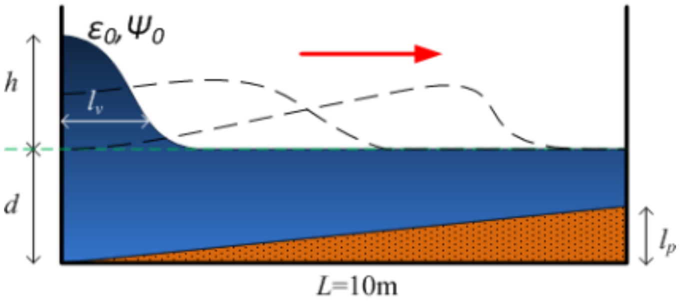

Fig. 3. Static Gaussian profile.

Finally, considering the velocity potential Ψ as known, we can generate the time varying profiles of breaking waves as a function various parameter (slope of the seabed, water depth, ...), see figure 4. The shape of sea surfaces is now supposed to be given and boils down to smooth deterministic curves.

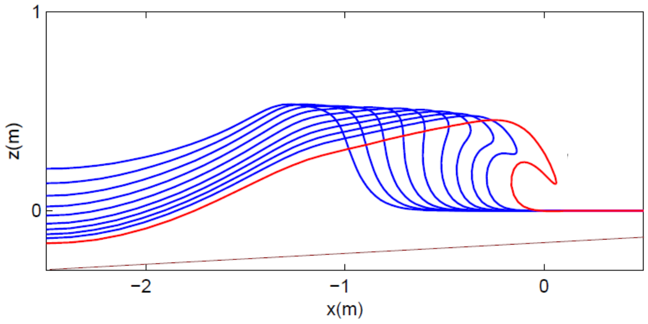

Fig. 4. Breaking wave profiles.

B. *Electromagnetic scattering modeling*

As in the case of linear sea surfaces, the scattering by breaking waves treated as smooth curves could a priori be modeled by a standard Method of Moments (MoM). Unfortunately, the breaking wave profile has strong local curvatures, see figure 5 and significant cavity, see figure 6. And it is now well known that important local curvatures and cavities involve severe convergence problems for the MoM [6], [7].

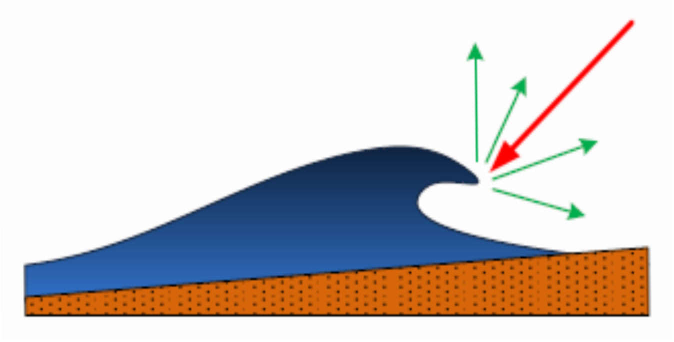

Fig. 5. Scattering by the high curvature of the sea wave profile.

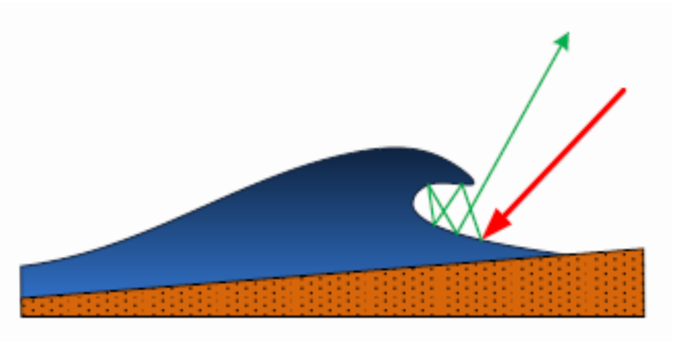

Fig. 6. Scattering by the cavity of the sea wave profile.

A very common solution for high curvature problem consists in combining Mom with ray theory [8], [9]. Nevertheless, this approach requires an arbitrary split between the both theories and remains non-relevant for cavities. In previous studies, we investigated higher order MoM [10] and Adaptive Multiscale Moment Method [11]. In this paper, we consider an Adaptive Finite Element approach [12]. For the seek of simplicity, the sea water is assumed to be an homogeneous dielectric medium whose permittivity is a complex function that depends on the salinity and the EM frequency, see figures 7.

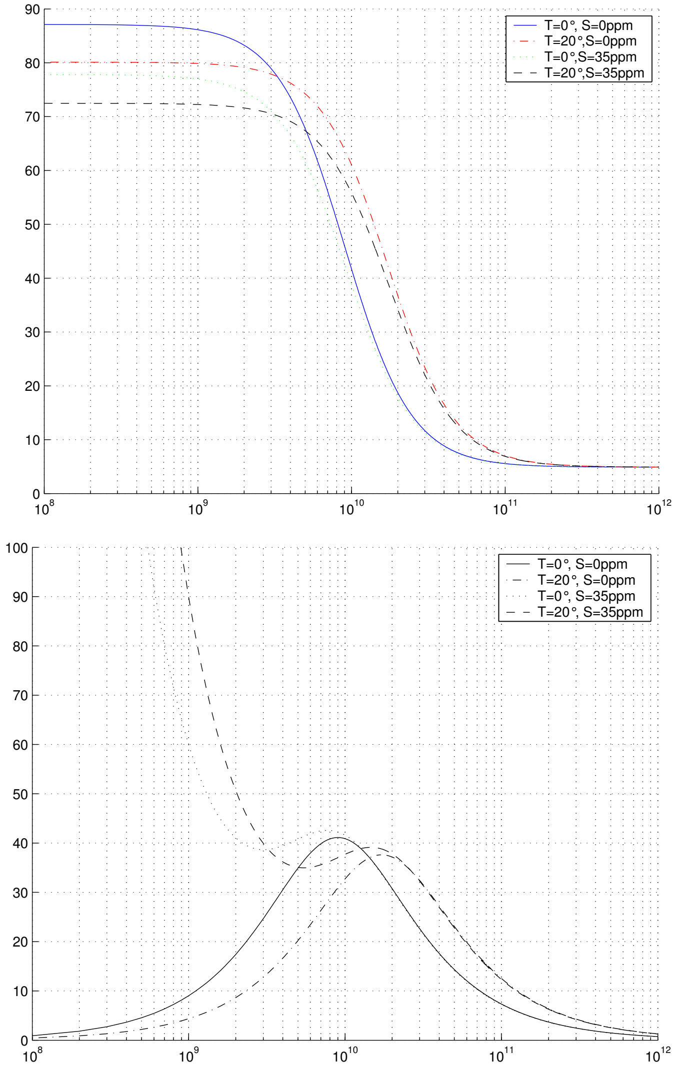

Fig. 7. Real and Imaginary part of the relative permittivity of the pure and the salt (35ppm) water.

The electric field satisfies the Helmholtz equation:

$$\nabla \times \left(\nabla \times \vec{E}\right) - k^2 \vec{E} = 0 \tag{1}$$

where $k = \omega\sqrt{\varepsilon\mu_0}$. In the present case, ε is equal to ε_0 above the surface and ε_{sea} in the sea.

In the present case, the incident electric field is a plane incident wave:

$$\vec{E}\left(\vec{x}\right) = \vec{E}_0 \cdot e^{\vec{k}\cdot\vec{x}} \tag{2}$$

where $\vec{k} = (k \cdot \sin\theta_0, -k \cdot \cos\theta_0)$ and θ_0 is the angle of incidence.

1) Infinite elements: Since the scattering problem is an exterior Maxwell problem, we truncate the exterior domain with a sphere $S_a = \{|\vec{x}| = a\}$ surrounding the crest of the breaking wave. The global domain Ω is split into a near-field domain $\Omega_a = \{|\vec{x}| < a\}$ and a far-field domain $\Omega^a = \{|\vec{x}| > a\}$, see figure 8.

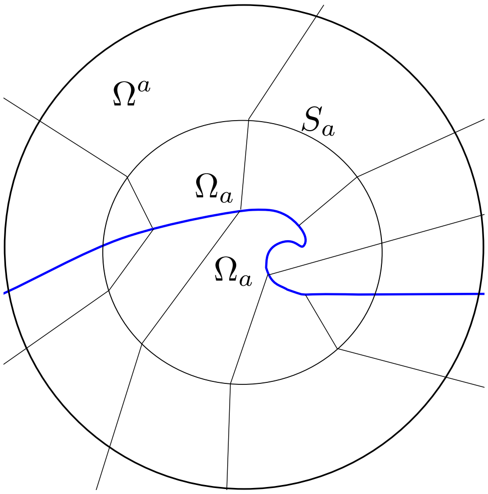

Fig. 8. Schematic presentation of the infinite elements.

The far-field domain is split into regular homogeneous infinite elements. Some of them are characterized by the permittivity of the void (ε_0) and the other are characterized by the permittivity of the sea water (ε_{sea}).

2) hp-Adaptivity: The near-field domain is meshed by Nedelec's triangular elements where the scale of the elements is denoted h. Each element is approximated by a polynomial of degree p. The automatic hp-adaptivity is based upon the projection-based interpolation. The optimal mesh is obtained by minimizing the interpolation error. This minimization is estimated locally and computed step by step. Finally, this algorithm delivers optimal h-convergence and p-convergence, see figure 9.

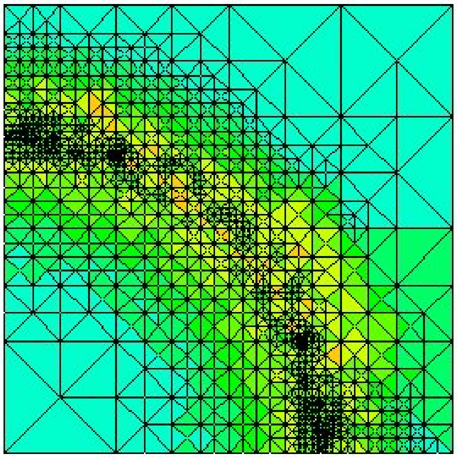

Fig. 9. Mesh refinement in the vicinity of a curved boundary.

III. NUMERICAL SIMULATIONS

Among all the time varying profiles generated by the fluid mechanic theory, several of them are selected for the numerical simulations, see figure 10.

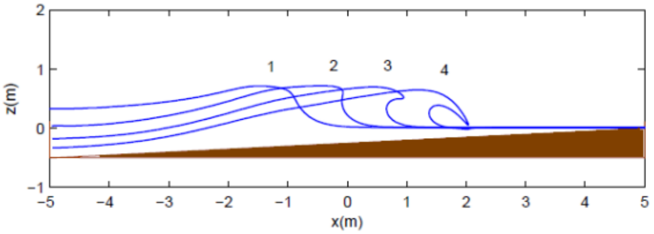

Fig. 10. Simulation for selected profiles.

The figure 11 shows the Radar Cross Section (RCS) for 3 different profiles in L-Band (1.5 GHz) and in vertical polarization. These numerical simulations are obtained using more than 2500 triangular vertex elements. The RCS is computed for different incident angles θ_0.

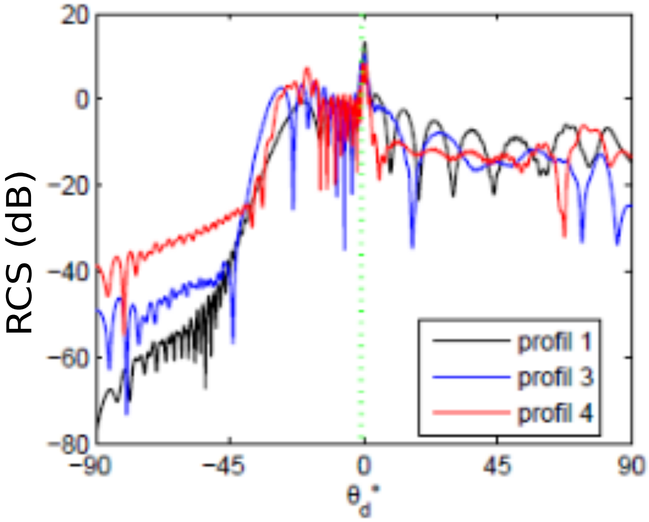

Fig. 11. Radar Cross Section for normal incident EM wave in vertical polarization.

To precisely analyze the distribution of the scattered field in the vicinity of the breaking wave crest, figures 12, 13 and 14 represent the local cartography in this area for three different angles of incidence. The scattering by the crest and the resonance modes in the cavity clearly appears.

IV. CONCLUSION

First and foremost, the hp-Adaptive Finite Element Method is proved to be an efficient approach to treat the problem of the scattering by a breaking waves. Moreover, the automatic vertex decomposition induced by the adaptive process in this case could be an interesting tool for qualitative interpretations of the radar signature related to a breaking wave. Finally, this study will be continued and extended to simulated the radar signature of inhomogeneous breaking waves. Indeed, the

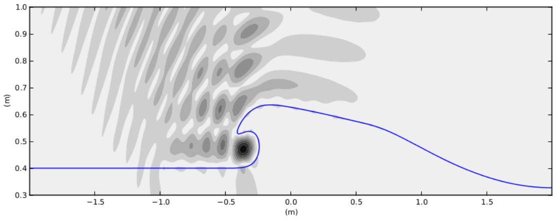

Fig. 12. Cartography of the scattered field for tilted incident EM wave in vertical polarization($\theta = 45°$).

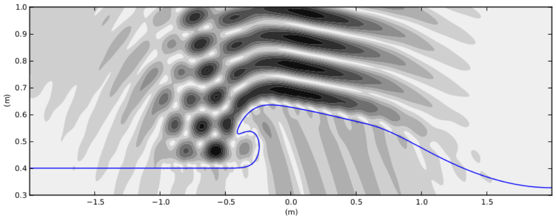

Fig. 13. Cartography of the scattered field for normal incident EM wave in vertical polarization ($\theta = 0°$).

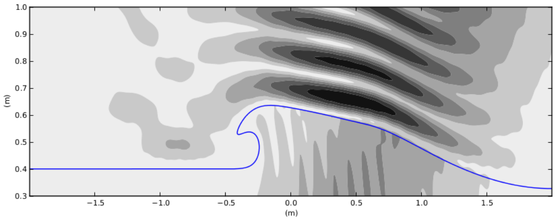

Fig. 14. Cartography of the scattered field for tilted incident EM wave in vertical polarization($\theta = -45°$).

whitening effects (mixture between salt water and air) need to take into account non-homogeneous sea water for simulations.

REFERENCES

[1] Q. Ma, Ed., *Advances in Numerical Simulatio of Nonlinear Water Waves*, ser. Advances in coastal and ocean engineering. World scientific, 2010, vol. 11.

[2] C. Alves, “On the choice of source points in the method of fundamental solutions,” *Engineering Analysis with Boundary Elements*, vol. 33, no. 12, p. 13481361, 2009.

[3] Y. Cao, W. Schultz, and R. Beck, “A three-dimensional desingularized boundary integral method for potential problems,” *International Journal Numerical Method in Fluids*, vol. 12, no. 8, p. 785803, 1991.

[4] D. Young, W. Hwang, C. Tsai, and H. Lu, “Accuracy of desingularized boundary integral equations for plane exterior potential problems.” *Engineering Analysis with Boundary Elements*, vol. 29, no. 3, p. 224231, 2005.

[5] Y. M. Scolan, “Some aspects of the flip-through phenomenon: A numerical study based on the desingularized technique,” *Journal of Fluids and Structures*, vol. 26, pp. 918–953, 2010.

[6] C. Davis and K. Warnick, “Error analysis of 2-D MoM for MFIE/EFIE/CFIE based on the circular cylinder,” *Antennas and Propagation, IEEE Transactions on*, vol. 53, pp. 321 – 331, 2005.

[7] R. Khairi, A. Coatanhay, and A. Khenchaf, “Optimal high-order method of moment combined with NURBS for the scattering by a 2D cylinder.” *Advanced Electromagnetics*, vol. 2, no. 1, pp. 33–43, 2013.

[8] F. Molinet, “Edge-excited rays on convex and concave structures: a review,” *Antennas and Propagation Magazine, IEEE*, vol. 47, no. 5, pp. 34 – 46, oct. 2005.

[9] ——, “Uniform asymptotic solution for the diffraction by a discontinuity in curvature,” *Annales Des Télécommunications*, vol. 50, pp. 523–535, 1995.

[10] R. Khairi, A. Coatanhay, A. Khenchaf, and Y.-M. Scolan, “Numerical modeling of electromagnetic waves scattering from 2D coastal breaking sea waves.” *European Physical Journal in Applied Physics*, vol. 64, no. 2, pp. 24 505–24 510, 2013.

[11] A. Coatanhay and Y.-M. Scolan, “Simulation of the electromagnetic scattering by coastal breaking sea waves in l-band using adaptive multiscale moment method,” in *WISE*, Huatulco, Mexico, 2013.

[12] L. Demkowicz, *Computing with hp-Adaptive Finite Elements*, ser. Applied Mathematics and non-linear science series. Chapman & Hall/CRC, 2007, vol. 1.

[13] A. Awada, M. Ayari, A. Khenchaf, and A. Coatanhay, “Bistatic scattering from an anisotropic sea surface: Numerical comparison between the first-order ssa and the tsm models,” vol. 16, no. 3, pp. 383–394, 2006.

[14] Y. Ayari, A. Khenchaf, and A. Coatanhay, “Bistatic scattering by sea surface at large incident angles : Two scame model using the unified sea spectrum,” *Journal of Applied Remote Sensing*, vol. 1013532, pp. 1–19, 2007.